Onset of turbulence in accelerated high-Reynolds-number flow

Ye Zhou, Harry F. Robey, and Alfred C. Buckingham
Lawrence Livermore National Laboratory, University of California, Livermore, California 94551
(Received 3 June 2002; revised manuscript received 11 October 2002; published 14 May 2003)

A new criterion, flow drive time, is identified here as a necessary condition for transition to turbulence in accelerated, unsteady flows. Compressible, high-Reynolds-number flows initiated, for example, in shock tubes, supersonic wind tunnels with practical limitations on dimensions or reservoir capacity, and high energy density pulsed laser target vaporization experimental facilities may not provide flow duration adequate for turbulence development. In addition, for critical periods of the overall flow development, the driving background flow is often unsteady in the experiments as well as in the physical flow situations they are designed to mimic. In these situations transition to fully developed turbulence may not be realized despite achievement of flow Reynolds numbers associated with or exceeding stationary flow transitional criteria. Basically our transitional criterion and prediction procedure extends to accelerated, unsteady background flow situations the remarkably universal mixing transition criterion proposed by Dimotakis [P. E. Dimotakis, J. Fluid Mech. **409**, 69 (2000)] for stationary flows. This provides a basis for the requisite space and time scaling. The emphasis here is placed on variable density flow instabilities initiated by constant acceleration Rayleigh-Taylor instability (RTI) or impulsive (shock) acceleration Richtmyer-Meshkov instability (RMI) or combinations of both. The significant influences of compressibility on these developing transitional flows are discussed with their implications on the procedural model development. A fresh perspective for predictive modeling and design of experiments for the instability growth and turbulent mixing transitional interval is provided using an analogy between the well-established buoyancy-drag model with applications of a hierarchy of single point turbulent transport closure models. Experimental comparisons with the procedural results are presented where use is made of three distinctly different types of acceleration driven instability experiments: (1) classical, relatively low speed, constant acceleration RTI experiments; (2) shock tube, shockwave driven RMI flow mixing experiments; (3) laser target vaporization RTI and RMI mixing experiments driven at very high energy density. These last named experiments are of special interest as they provide scaleable flow conditions simulating those of astrophysical magnitude such as shock-driven hydrodynamic mixing in supernova evolution research.

DOI: 10.1103/PhysRevE.67.056305 PACS number(s): 47.27.Ak, 47.27.Cn

I. INTRODUCTION

Our principal contribution here is the development of a turbulent mixing transitional criterion and a procedure for modeling and predicting the required time interval to achieve transition when the background flow is unsteady rather than stationary. We submit that such a criterion and estimation procedure is essential for analysis, experimental design, and diagnostic development. Emphasis is on studies of extremely energetic, high pressure, supersonic, high-Reynolds-number flow environment of current and continuing interest. Considered are applications in supersonic combustion, hypersonic aerothermodynamic design, and astrophysical stellar and planetary evolution research, among others. Specific emphasis here is given to research on the evolution of turbulent mixing states originating with accelerated flow instabilities such as RTI (Rayleigh-Tailor instability) [1,2] or RMI (Richtmyer-Meshkov instability) [3,4]. The researcher needs to conceptually bridge the significant transitional flow interval separating the initial accelerated unstable flow conditions [5–7] from their potential evolution into fully developed turbulence [8–11]. The investigator charged with design or analysis of experiments in a supersonic, high energy flow facility must determine the energetic drive duration (shock tube length, diameter and drive energy density, or laser pulse sequencing, for example) to ensure that mixing transition may be reliably attained during a test interval of unsteady background flow. The attendant problem of diagnostics design and implementation capable of recording a sufficient sequence of flow realizations for experimental verification also demands reliable estimates of mixing transition time. In this paper we introduce the development, implementation, and test of a criterion and model procedure which provides this information for accelerating, unsteady, compressible, high-Reynolds-number flows.

To avoid ambiguity here we define fully developed turbulence as the concluding state of flow evolution which results in a statistically random distribution of velocity and state variable (such as density and temperature) perturbations within a mean transient or stationary background flow and thermodynamic state. The concluding flow and state perturbations must reach sufficient intensity and persistence so as to excite all state-permissible, statistically distributed degrees of dynamic freedom.

The physical space visualization of turbulence may be recognized as a randomly distributed, seemingly disorganized but dynamically connected continuum array of filamentary structures of all size scales with intermittently changing boundaries and topological features. However, Fourier transformation of physical space observations reveals the universal spectral characteristics of fully developed turbulence. One such spectral characteristic of onset and

eventual attainment of fully developed turbulence is the growth and establishment of a Reynolds-number dependent inertial range separation in the universal turbulent energy spectrum [12,13]. This inertial range separation is the transfer bridge for energy cascade from the larger scales of motion where it is produced down to the smallest motion scales where it is dissipated. In reality, of course, the energy cascade is not unidirectional. Complete description includes the well-established (but often neglected) reverse cascade of high frequency energy that is backscattered towards the larger production scale motions [14]. An important consequence of this inertial range separation is the isolation, hence lack of direct influence of the dynamics of the largest scales of motion on the smallest dissipation scale dynamics which are governed almost solely by molecular transport processes. Implicit in our procedure is development of a scale interaction model for estimating the time interval sufficient for establishing this inertial range separation.

In our present work we generalize the mixing transition criteria proposed by Dimotakis [15] to include time development of the mixing transition. One notes that establishing the time dependence and a general interval for mixing transition to turbulence from the beginning of instability growth is not generally feasible, since the outer-scale Reynolds number and the foregoing key length scales may individually evolve with time as well as with variation in flow conditions. However, once the time dependence of the driving inertial flow field is established (such as is the case for RTI and RMI initiated flows) our procedure provides reasonable estimates of the time duration necessary for mixing transition to fully developed turbulence.

Many predictions of RTI and RMI initiation and subsequent history of the instability growth are based on the application of one of the variations of the familiar buoyancy-drag model [16–18]. These model predictions often illustrate general features whose details are usually traced in numerical simulations. The buoyancy-drag models have been shown [19–23] to provide faithful representations of the early time instability growth and material penetration phases in direct comparison with the experimental evidence in their more refined and carefully applied versions. In cases where a single length scale dominates, we illustrate here a parallel between the buoyancy-drag models and a one-equation turbulence transport closure model [24,25]. We consider this parallel in suggesting application of standard engineering transport models for calculating the evolution of turbulent mixing of the RTI and RMI initiated flows after turbulence onset. Our analysis here suggests that once the mixing region becomes turbulent, two-equation transport equations describing the evolution of both spatial and temporal scales are required to achieve even minimally accurate description of turbulent transport and multifluid mixing (see, for example, Ref. [26]).

The paper is arranged as follows. First we discuss the background and development of a procedure for estimating the time required for mixing transition to turbulence when the background flow is nonstationary. Next, for comparison, we apply the procedure to three classes of RTI and RMI experiments: (1) a classical low speed RTI experiment [27]; (2) shock tube initiated RMI experiments [28]; and (3) laser driven high energy density RTI experiments [29]. Some novel features and issues arising in the laser driven experiments demand special consideration, evaluation, and analysis. The bulk of this latter discussion appears in separate papers [29,30]. Next we describe some of the dominant influences of compressibility on transitional and developed turbulent mixing generally and their consideration in developing the unsteady transitional criterion and procedural model specifically. In a subsequent section we will illustrate a parallel to the buoyancy drag-model with single point closure transport models, beginning with a prototypical one-equation, single point, turbulent transport closure model, followed by subsequent examination of more general single point transport model closure schemes.

We complete the present paper with a summary and conclusions.

II. PREDICTED TIME INTERVAL FOR MIXING TRANSITION TO TURBULENCE

A key in establishing the necessary time needed for achieving mixing transition to turbulence is to understand the physical relationship between several important length scales. These length scales emerge in part from analysis of the governing Navier-Stokes equation, conservation of energy, conservation of mass, and the classical statistical fluid dynamic (Kolmogorov) representation of turbulent flow [8–11]. The principal length scales under consideration include the following.

Length scale 1, The outer scale, δ. The largest dynamic flow length scale at which the external forcing (the drive which produces both the overall background flow kinetic energy and the kinetic energy of the turbulent fluctuations) is in action.

Length scale 2, Dissipation (Kolmogorov) scale, λ_k. The smallest dynamic flow length scale (microscale) at which the continuum fluid turbulent kinetic energy dissipates in excitation of molecular scale motions. This is the limiting or smallest length scale at the boundary between turbulent continuum motion and the molecular scale motions, represented on the average by the Boltzmann collision integral averaged transport properties.

The classical Kolmogorov theory [8–11] assumes that in the inertial subrange, the dynamics at an intermediate scale, λ, cannot be influenced by the outer, low frequency scales, δ, where turbulent energy is produced, nor can it be influenced by the inner, high frequency, viscous dissipation scales [represented by the Kolmogorov microscale, $\lambda_K=(\nu^3/\varepsilon)^{1/4}$, where ν is the kinematic viscosity and ε is the dissipation rate of the turbulent kinetic energy].

$$\lambda_K \ll \lambda \ll \delta.$$

The outer-scale Reynolds number

$$\mathrm{Re}=\frac{U\delta}{\nu}$$

must be defined carefully. It depends on the types of the flow field. Here U is the characteristic velocity.

Length scale 3. The Taylor microscale λ_T. Another microscale having special utility is the Taylor microscale λ_T somewhat larger than the Kolmogorov microscale previously introduced. This microscale is directly related to the turbulent statistical velocity autocorrelation function. It has a special identity and role in analysis and simulation of turbulent flow statistical structure [8–11].

A. Mixing transition threshold proposed by Dimotakis for stationary flows: A review

Recently, Dimotakis [15] assessed a large number of experiments and concluded that mixing transition occurs in shear layers, jets, Couette-Taylor flows, and other stationary flows when a novel Reynolds-number threshold for mixing transition was reached. The comparisons suggested that it may be regarded as a nearly universal phenomenon signalling attainment of turbulent mixing transition. Dimotakis pointed out that the mixing transition threshold reflects the inability of the flow to remain stable as the damping effects of viscosity are reduced with increasing Reynolds number. Furthermore, the mixing transition occurs at Reynolds numbers beyond the classical velocity field transition and represent a subsequent, often well-identified, transition in the flow [15]. For all these flows, visualization illustrates that the mixing transition is rather abrupt and results in an increasingly disorganized three dimensionality and sudden increase in atomically mixed material.

The transition to a well-mixed state for jets, shear layers, boundary layers, and Couette-Taylor flows illustrates qualitatively different behavior below and above a narrow range of Reynolds numbers. Dimotakis found that for all of these flows, the resulting fully developed turbulent flow requires that an outer-scale Reynolds number of $\mathrm{Re} \geqslant 1\text{–}2\times 10^4$, or a Taylor microscale Reynolds number of $\mathrm{Re}_T \geqslant 100\text{–}140$ must be attained. Furthermore, mixing transition appeared in the extensive survey of stationary flows to be almost independent of the details of the flow geometry. Dimotakis [15] noted that the mixing transition coincides with the appearance of the inertial range.

The mixing transition threshold proposed by Dimotakis for stationary flows marks a significant advance in refining and narrowing the Reynolds-number criterion for predicting mixing transition to fully developed turbulence. Dimotakis [15] illustrated that in the case of shear layers, U is taken as the constant free-stream velocity difference and δ is taken as the local depth of the shear layer (or, in the case of a chemically reacting shear layer, the local depth of the reaction zone within the shear layer). In the case of round, turbulent jets, U is taken as the local centerline velocity of the jet while δ is taken as the local jet diameter. He pointed out that the characteristic flow structural difference between shear layers and jets and their dependence on local values, is of interest in the context of spatially developing flows and the evolution of the distribution of scales and turbulence spectra.

The energy spectral interval of the complete Kolmogorov inertial range is usually too broad to be of practical use in experimental designs. To fix a tighter bound, Dimotakis proposed that the extent of the effective inertial range influence barrier can be narrowed to

$$\lambda_\nu < \lambda < \lambda_L ,$$

where two new length scales can be deduced from the Taylor and dissipation microscales.

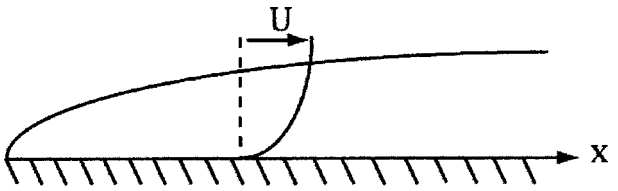

FIG. 1. Sketch of the development of a laminar viscous boundary layer on a flat plate.

Length scale 4. The inner viscous scale λ_ν. This may be estimated [15] as a multiple of the Kolmogorov microscale by inspecting the high-Reynolds experimental data compiled by Saddoughi and Veeravalli [13], $\lambda_\nu \approx 50\lambda_K \approx 50\delta\,\mathrm{Re}^{-3/4}$.

Length scale 5. The Liepmann-Taylor scale λ_L. This is the upper limit of the microscale mixing range [15]. With δ representing the outer laminar vorticity growth thickness, it is related to the Taylor correlation microscale λ_T. Based on the experimental data, Dimotakis [15] determined that $\lambda_L = 5\lambda_T$, where $\lambda_T = \delta\,\mathrm{Re}^{-1/2}$. In nondimensional form,

$$\frac{\lambda_\nu}{\delta} \approx 50\,\mathrm{Re}^{-3/4} < \frac{\lambda}{\delta} < \frac{\lambda_L}{\delta} \approx 5\,\mathrm{Re}^{-1/2}.$$

The criterion for mixing transition to turbulence can be determined only by the outer-scale Reynolds numbers, for a given outer scale δ. The insight offered by Dimotakis [15] provides guidance for future experimental designs directed to achieving mixing transition in a wide range of stationary flows.

B. New mixing transition threshold proposed for time-dependent flows

The mixing problem for many applications is a transitional problem. For high energy density physics applications, such as experiments on lasers and Z pinches, flows start from rest at $t=0$. In high-Reynolds-number flows of short time duration, the Taylor microscale may not have sufficient time to reach its asymptotic value.

The Taylor microscale (for stationary, homogeneous, isotropic flow) depends on the integral scale δ and the Reynolds number as $\lambda_T \sim \delta\,\mathrm{Re}^{-1/2}$. This is analogous to the development of a laminar viscous boundary layer on a flat plate $\lambda \sim X\,\mathrm{Re}^{-1/2}$ (see Fig. 1). For time-dependent viscous flows, classical similarity governs the outer-scale growth rate as follows.

Length scale 6. Growth rate of an outer-scale viscous shear layer scale λ_D. For time-dependent flows, we need to consider an additional scale, a growth rate scale. This is provided by the growth rate of an outer-scale viscous shear layer. We take this to represent the basic scale length growth

rate of shear generated vorticity. In our procedure this is given by the classical viscous layer similarity growth rate on a solid surface accelerated initially from rest. This similarity form for viscous shear layer growth was first identified nearly 150 yr ago and independently confirmed in several classical 19th century theoretical studies (Stokes [31], Rayleigh [1], Lamb [32]). The temporal development of such a laminar viscous layer is well known to vary as $(\nu t)^{1/2}$ [1,10,31,32],

$$\lambda_D \equiv C(\nu t)^{1/2}.$$

Here the coefficient of the diffusion layer, C, was suggested as $\sqrt{15}$ for isotropic, homogeneous turbulence [10], as four for unsteady parallel flows [33], and as five for boundary layer (following the Liepmann-Taylor constant by Dimotakis [15]).

For unsteady mixing transitional flows of interest here, we generalize the proposal of Dimotakis based on the following three observations.

(i) The outer scale δ and the outer-scale Reynolds numbers are both functions of time.

(ii) The least upper bound of the developing inertial range influence barrier is the minimum of the Liepmann-Taylor scale λ_L and laminar viscous scale λ_D: $\lambda_{\min} \equiv \min[\lambda_L, \lambda_D]$.

(iii) The greatest lower bound of the inertial range influence barrier is the developing inner viscous scale λ_ν.

The inequality just introduced provides a sufficient condition for estimating a mixing transition criterion for unsteady transitional flows, viz.,

$$\lambda_{\min} > \lambda_\nu.$$

For time-dependent transitional flows, mixing transition is achieved when a range of scales exists such that the temporally developing least upper bound is significantly larger than the temporally developing greatest lower bound. In the presence of a sufficient Reynolds number an additional interval of time is required to generate the scales needed for a mixing transition [$\mathrm{Re} > (1\text{–}2)\times 10^4$ and $t > t_C(\lambda_{\min}, \lambda_\nu)$].

Dimotakis [15] has made use of the classic viscous similarity transform in space; our application is in time. In either application, the temporal similarity transform is unique for viscous flows. There are no others. Its origin is in the mid-19th century as we noted already. Its application to mixing transition in the temporal sense is our contribution.

Care must be taken to properly compute the transport properties, particularly viscosity [34] and for multifluid flows, the diffusivity [35] at material interfaces in multifluid mixing. Additional emphasis has been given to astrophysical flow situations and laser target interaction experiments designed to create flow conditions which can mimic them with appropriate scaling. Here the plasma influences on the fluctuating fluidynamic field transport properties on calculated scale growth are subjects of present and continuing experimental and theoretical research in these intensely energetic applications ([29,36,37]).

We emphasize here flow situations where the explicit time dependence of the driving flow has been determined theoretically and experimentally. This is a necessary first requirement in order to advance our procedure for application to a more general class of transitional mixing flow situations. In this regard, the time dependence of $\mathrm{Re}(t)$, $\lambda_\nu(t)$, $\lambda_L(t)$, and $\lambda_D(t)$ have intrinsic and independent dependence on developing outer flow conditions so that no universally applicable criterion in terms of arbitrary time dependence of the outer scale can be obtained.

C. Application of time-dependent mixing transition to RTI and RMI induced flows

For the RTI and RMI induced flows, the outer-length scale δ is uniquely identified (Cook and Dimotakis [38]) as the mixing zone extent, h. The velocity U is given by its growth rate $\dot{h}$. Indeed, we stress that this mixing zone length scale is aligned with the flow vector rather than perpendicular to it as in the case of the previously described shear layers. We offer a few remarks on the significance of this flow aligned scale growth in RT and RMI investigations.

We note that the instability growth eigenvalues in the outer RTI and RMI acceleration driven flows are components aligned with the acceleration vector. They are uniquely characterized by streamwise component instability scales, in distinct contrast to supplemental scale growth in normal or lateral directions. These scales characterize the later developing, secondary, shear-driven instabilities. In the classical RTI theory only the distribution of streamwise amplitudes appear as initial perturbation conditions. The orthogonal dimensions and shape factors are parametrically imposed initial conditions on spatial frequency with periodic boundary conditions [5]. In effect, parametric variation of initial amplitudes and distributions in model calculations provide for systematic investigation of the influence of material interface surface roughness on the actual physical situations under study. Of course, prediction of the growth of the scales developing orthogonally to the streaming coordinate in the secondary, later developing, shear layers, and particularly the evolution of critical microscales within them, and their relation to the overall ''clock time'' associated with the outer background acceleration driven scale δ, are implicitly considered in our procedure.

We now illustrate the time dependence for a specific flow in which we know (from measurement or simulation) the time history of the outer flow. The heavy fluid is denoted by $i=s$ (spikes) and the light fluid is denoted by $i=b$ (bubbles). We identify the length scale δ with average amplitude or depth of the turbulent material mixing zone

$$h(t) = h_b(t) + h_s(t).$$

For example, for the case of RTI flow, we know how the outer scale develops as a function of time, and therefore, how the outer-scale Reynolds number depends on time. which satisfies the scaling law [39]

$$h_i(t) = \alpha_i A g t^2.$$

Note that $\alpha = \alpha_s + \alpha_b$ is the sum of two constants.

The Atwood number is given by

$$A=\frac{\rho_1-\rho_2}{\rho_1+\rho_2}.$$

Using the form introduced in Zhou [40], the scaling law for the RMI flows is

$$h_i=\frac{K_0^{3/2}}{\varepsilon_0}\left\{1+(C_{\varepsilon 2}-1)\frac{\varepsilon_0}{K_0}t\right\}^{\theta_i},$$

where $C_{\varepsilon 2}$ is a constant. K_0 and ε_0 are the initial values of turbulent kinetic energy and dissipation rate. Some theoretical analysis estimated the values of θ_b to be between 2/3–7/12 (Zhou [40]). Shvart *et al.* suggested values for the exponent θ_b are 0.4 for 2D [41] and 0.2–0.25 for 3D [42,43]. Other studies reported the values of θ_b to be 2/3 (Barenblatt [44], Youngs [45], Ramshaw [46]). For an initial condition where the multiple length scales are reduced to a single dominant length scale, we have

$$h_i=L_0\left\{1+(C_{\varepsilon 2}-1)\frac{V_0}{\sqrt{2}L_0}t\right\}^{\theta_i}.$$

Shvarts *et al.* [42] presented a detailed discussion on the scaling of nonlinear RMI (as well as RTI) in two and three dimensions. They argued that the RMI mixing zone is characterized by two distinct scales t^{θ_b} and t^{θ_s} for the bubble and spike front respectively, with $\theta_s/\theta_b\approx 1+A$ for both two and three dimensions. The θ_b is found to be 0.2 for 3D [43]. Clark and Zhou [47], on the other hand, have argued that $\theta_b=\theta_s\equiv\theta$, but with different time origin.

For RTI driven flow, we find that, by substituting $\mathrm{Re}=2(\alpha Ag)^2t^3/\nu$, the condition for the mixing transition indicates $\lambda_D(t)<\lambda_L(t)$ (i.e., temporally limited flow development),

$$C(\nu t)^{1/2}>50\delta\,\mathrm{Re}^{-3/4},$$

which gives the condition

$$t_T>\frac{1}{2}\left(\frac{50}{C}\right)^{4/3}\nu^{1/3}(\alpha Ag)^{-2/3}$$

for achieving mixing transition in RTI driven flows. For the case of $\lambda_D(t)>\lambda_L(t)$ (essentially the stationary flow limit of the Liepmann-Taylor scale), however, we demand that

$$\lambda_L(t)=5\,\mathrm{Re}^{-1/2}\delta>\lambda_\nu=50\delta\,\mathrm{Re}^{-3/4}.$$

As a result, the critical time for achieving mixing transition becomes

$$t_T>10\times 5^{1/3}\nu^{1/3}(\alpha Ag)^{-2/3}.$$

The conditions of the flow, such as the Atwood number, viscosity, and acceleration, determine which condition should apply.

Following the same procedure, we can estimate the time required for achieving mixing transition for an RMI driven flow. For simplicity, we take the late time limit and assume $\theta_s=\theta_b$ so that

$$\delta=h\approx\gamma t^{\theta_b},$$

which is applicable for both multiple length scales case

$$\gamma\equiv 2\left\{(C_{\varepsilon 2}-1)\frac{K_0^{(3-2\theta_b)/2\theta_b}}{\varepsilon^{(1-\theta_b)/\theta_b}}\right\}^{\theta_b}$$

or single dominant length scale case

$$\gamma\equiv 2\left\{(C_{\varepsilon 2}-1)\frac{V_0L_0^{(1-\theta_b)/\theta_b}}{\sqrt{2}}\right\}^{\theta_b}.$$

Now the outer-scale Reynolds number is

$$\mathrm{Re}=\frac{h\dot{h}}{\nu}\approx\frac{\theta_b\gamma^2t^{2\theta_b-1}}{\nu}.$$

For the temporally limited flow development case, we have

$$t_T>\left\{\frac{50\nu^{1/4}}{C\theta_b^{3/4}\gamma^{1/2}}\right\}^{4/(2\theta_b-1)},$$

while for the stationary flow limit of Liepmann-Taylor scale, we find

$$t_T>\left\{10^4\frac{\nu}{\theta_b\gamma^2}\right\}^{1/(2\theta_b-1)}.$$

For the RTI and RMI driven flow, the Kolmogorov scale and the Taylor microscale are also time dependent (straightforward so not shown to limit the length of the paper):

$$\lambda_K=h(t)\mathrm{Re}^{-3/4}\propto t^{-1/4}$$

and

$$\lambda_T(t)\approx h(t)\mathrm{Re}^{-1/2}\propto t^{1/2}.$$

The corresponding Reynolds number based on the Taylor microscale is given by $R_\lambda\approx\mathrm{Re}^{1/2}\propto t^{3/2}$.

The turbulent kinetic energy and dissipation rate are the two most important quantities in turbulence modeling [24,25]. Here the turbulent kinetic energy can be estimated as proportionately time dependent

$$K\approx\left(\frac{dh}{dt}\right)^2\propto t^2,$$

and from dimensional considerations the dissipation rate goes as

$$\varepsilon\approx\frac{(dh/dt)^3}{h}\propto t.$$

The turbulence length scale, defined from these two measurements as, $K^{3/2}/\varepsilon$, clearly reduces to the t^2 scaling. The turbulence time scale, defined by K/ε, is about $h/(dh/dt)=t/2$.

Sadot *et al.* [48] have proposed an alternative growth law encompassing the linear, early nonlinear (see also the impor-

tant theory by Zhang and Sohn [49]), and later, pretransitional, asymptotic instability behavior of bubble and spike amplitude. Recently, Jacobs and Krivets [28] reported that the model by Sadot *et al.* [48] provides excellent agreement with the Mach 1.3 shocktube experiment. The model amplitude consists of both an inverse tangent function and a natural log and can be regarded as the outer scale δ when repeating our analysis here. For brevity, we will not carry out this straightforward calculation here.

III. ILLUSTRATIONS WITH EXPERIMENTAL COMPARISONS

We first consider a classical fluid dynamics experiment conducted at Cambridge University [27]. The referenced authors describe an experimental investigation of Rayleigh-Taylor instability between two miscible fluids. This experiment made use of a unique low-perturbation removal technique that minimized Kelvin-Helmholtz instability growth. The specific object of the experiment was the investigation of the gravitationally driven instability between salt and fresh water layers. The experimental apparatus was a tank with longitudinal and lateral dimensions of $200\times400\ \mathrm{mm}^2$ and a height of $H=500$ mm. The Atwood number is about 0.002. Since the Atwood number is low, the kinematic viscosity of water at room temperature, 0.01 cm^2/sec provides an appropriate viscous dissipation cutoff level. Dalziel *et al.* [27] reported that the flow is contaminated by the wake induced by the stainless steel barrier withdrawal at 10 sec. Assuming the late time similarity scaling, we found that the Reynolds number is just about 10^4. Therefore, if the test section could be enlarged sufficiently, the mixing transition induced by RTI, in principle, can be measured without the contamination of the wake.

We next examine some low Mach number shock tube experiments that provide encouraging evidence of our ability to predict mixing transition times. These experimental investigations of RMI flow development are usually carried out in shock tubes using elastic-plastic membranes to separate the two gases. However, the presence of these membranes, in addition to introducing other experimental problems, such as the introduction of unwanted material strength influences on the initial conditions, obstruct use of advanced visualization techniques such as planar laser induced fluorescence (PLIF). In recent years Jacobs and co-workers [28] have developed and successfully applied a new technique by which a perturbed gas-gas contact surface interface is created in the shock tube without having to resort to a separating membrane. A two-gas impingement stagnation plane of separation is created using two small slots on opposing sides of the shock tube walls. These act as injection inlets for the two gases flowing from opposing ends of the tube. A gentle rocking motion of the shock tube provides the initial perturbation in the form of momentarily stationary waves. In their studies, PLIF visualization has been implemented and digital images captured for a sequence of low Mach numbers ($M_s=1.107$, 1.207, and 1.3). The visualization (Fig. 2) yields very clear views of the instability growth [28]. The mixing width and

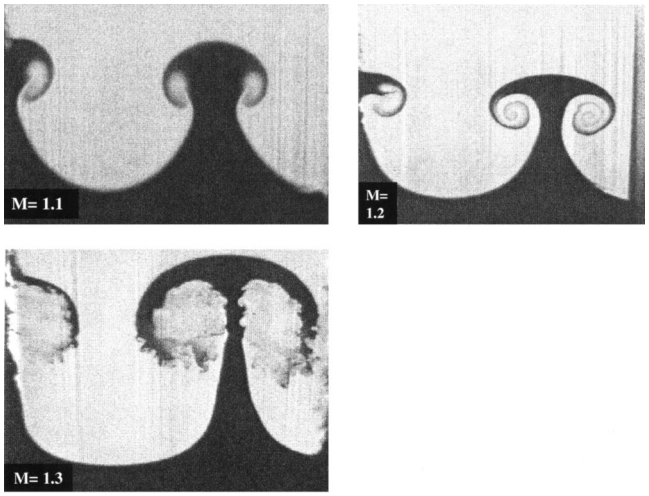

FIG. 2. PLIF images of RMI shock tube flow development at $t=6$ ms for incident shock Mach numbers: 1.1, 1.2, and 1.3 (from Ref. [28]).

Reynolds number for $M_s=1.3$ are given in Figs. 3(a) and 3(b), respectively.

Applying our procedure, we find that in the experiments at $M_s=1.107$ and $M_s=1.207$, our predictions and the experiments (as evident from the PLIF images which can be seen in Fig. 2) indicate that mixing transition does not take place during the duration of the experiments for these two Mach numbers (not shown). However, when the experimental Mach number is increased to 1.3, applying our procedure, we predict mixing transition may occur approximately at $t=2.5$ ms [Fig. 3(c)]. Supporting this, the PLIF image for the highest Mach number shows characteristically well developed turbulent flow mixing structure in the vorticity generation region of secondary flow beneath the contact interface. All PLIF images are captured at the same experimental time ($t=6$ ms) for comparison.

As noted previously, the third class of experiments are described and discussed in detail in a separate publication [29].

IV. INFLUENCES OF COMPRESSIBILITY

For the high-Reynolds number, high Mach number flows of particular interest in many of our current research interests, compressibility significantly and directly influences the outer scales, δ, the associated outer-scale Reynolds numbers, Re, and their growth rates, while indirectly influencing the inner scales through significant alteration to transport and state properties at these extremely energetic and highly compressed flow conditions.

The outer-scale direct influences are readily measured in the experiments concomitant with measured changes to flow state properties. They are also explicitly traced in the fully compressible numerical simulations currently applied to analyze and complement the experiments. However, to provide a fresh perspective on some of the more significant effects of compressibility on turbulent mixing layers and their potential influences on our unsteady mixing transition procedure we

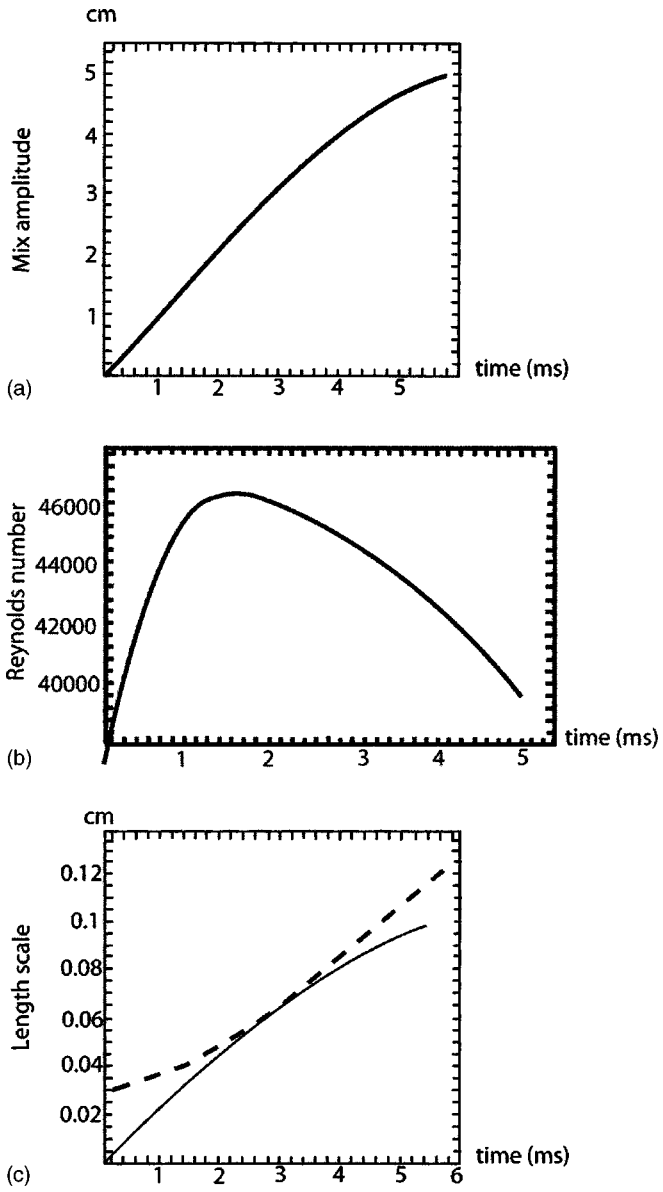

FIG. 3. (a) Temporal evolution of the mixing zone amplitude from a $M_s=1.3$ shock tube experiment based on a fit of the experimental data (Ref. [31]) $h=2[0.234+1.66\,\mathrm{Sinh}^{-1}(0.57t)]$. (b) RM outer-scale Reynolds number based on outer scale. (c) Comparison of the length scales for the RMI flow at $M_s=1.3$ (Solid line, temporally developing least upper bound; dash line, temporally developing greatest lower bound).

will briefly review some of the salient visible and experimentally verifiable features.

When transition to turbulence is attained in either compressible or incompressible flow, the visible mixing length scales undergo immediate and pronounced size increases over pretransitional (laminar) scales. For example, in stationary, wall-bounded shear mixing layers, the ratio of turbulent to laminar normal scale dimensions increases as a weakly exponential function of the characteristic outer-scale Reynolds number,

$$\delta(\text{turbulent})/\delta(\text{laminar}) \sim (1/14)\mathrm{Re}^{3/10},$$

Schlichting (Ref. [33]).

However, compressibility induces a significant reduction in the (spatial or temporal) *growth rate* of the outer, characteristic scales in comparison to their incompressible growth rate. This observable reduction in growth rate is a manifestation of the increasing (with increasing Mach number) competition between density variation influences on momentum and thermal energy dissipation in compressible shear layers. This predominately affects the outer, low frequency, flow scales, since most of the turbulent kinetic energy subject to this competition between momentum and thermal energy transport is produced and contained within the low frequency, large scale production end of the inertial range of the turbulent energy spectrum. This compressible flow competition between variable density and temperature changes in free shear layer mixing has stimulated considerable experimental attention. For example, the thermal and density variation competition and its influence on the dynamics of the large scale free shear layer flow structure has been systematically examined in the well-known studies of Brown and Roshko [50].

For wall-bounded, compressible shear layers, the reduction in growth rate has been found to have an inverse dependence on the square of the outer-flow Mach number. The approximate ratio of compressible to incompressible growth rates, based on a large number of experiments in air at low Mach number ($M<2.7$) is found to follow the scaling (Schlichting [33]),

$$(1+cb\mathrm{M}^2)^{-1}.$$

Here *cb* denotes the product of two dimensionless quantities: thermal recovery factor and shear stress coefficient. The product, *cb*, varies from about 1/10 to nearly unity depending on surface heat transfer, gas composition, and thermodynamic state.

A somewhat different Mach number dependence has been observed for the ratio of compressible to incompressible free shear layer growth rates at moderate flow Mach numbers. More recent experimental evidence indicates that the effective Mach number dependence should be based on the ''convective Mach number'' which is evaluated at the sound speed associated with the recovery temperature for the two interacting free shear streams and their relative velocities (Papamoschou and Roshko [51]). At higher Mach numbers, indications are that the ratio of compressible to incompressible growth rates for both bounded and free shear layers become asymptotic to a constant small value, *O* (1/5).

The direct, outer scale, compressibility influences are effectively isolated from the high frequency dissipation (microscale) range by the substantial inertial range associated with the usual high-Reynolds numbers of the experiments. Localized, high frequency, dissipation range influences of compressibility on the statistical velocity correlations are commonly approximated as near-infinitesimal corrections to the density-velocity product distributions. In recognition of the lack of an adequate experimental or direct numerical simulation data base (at the Reynolds numbers and Mach numbers of practical interest), this approximation is commonly applied, based partially on the assumption of very low

values (with respect to 1.0) of the characteristic Mach number of the ensemble averaged velocity fluctuations in conjunction with the negligibly low ratio of the averaged density fluctuations to the mean background density. This behavior is also predicted on the relatively large population of microscale dynamic encounters in the high frequency range which suggests a dynamic environment sufficiently dense in interactions to promote and maintain a reasonable approximation of a spatially homogeneous, near stationary statistical state. However, much more experimental evidence is sought, particularly, in decaying high Mach number turbulent flow to evaluate and improve our insight on microscale range insensitivity to direct effects of compressibility.

Our particular emphasis and attention here is given to the *Indirect* effects of high Mach number compressible flow and its influences on the microscale dissipation range cutoff of the energy spectrum and corresponding contraction of the inertial range. The critical quantities here are the high density, very high temperature transport properties, particularly viscosity and diffusivity, and the thermodynamic and partially ionized plasma composition states that develop in the high energy laser driven RTI and RMI experiments, and the supernova astrophysical events of primary interest to us. These influences and other issues affecting our procedure are evaluated and discussed in detail in the separately published experimental paper [29].

V. SCALING. PARALLELS BETWEEN BUOYANCY-DRAG AND SINGLE POINT CLOSURE MODELS

The buoyancy-drag model [16–18] is in common use for a description of the evolution of the mixed region material penetration boundaries in RTI and RMI driven flows [19–23]. The model equation represents the force balance consisting of three components: inertia, buoyancy, and Newtonian drag. The physical assumption inherent in the buoyancy-drag model is the existence of a single growing length scale, on the order of the thickness of the mixing zone itself, governing the dynamics of the mixing zone boundaries. Thus the model assumes that the large and growing length scale defined by the mixing layer thickness dominates the dynamics and that the effects of the small length scales can be ignored for the purpose of studying the bulk motion of the mixing layer [23]. The buoyancy-drag model has been developed with regard to acceleration driven hydrodynamic instabilities. It is instructive to view this in parallel with a length scale dominant single point closure transport model with attention to potential applications in transitional computations and analysis. To this end we make use of observations on the single point closure modeling hierarchy review by Speziale [24], by Wilcox [25], and more recently by Pope [11].

A. Before mixing transition with a single dominant scale

The typical buoyancy-drag model equation can be written in the following form:

$$\frac{dV_i}{dt}=\beta Ag-C_d\frac{\rho_i}{\rho_1+\rho_2}V_i|V_i|\frac{(\text{area})}{(\text{volume})}, \tag{1}$$

where $g(t)$ may represent either a constant (RTI) or an impulsive acceleration (RMI). The heavy fluid is denoted by $i=s$ (spikes) and the light fluid is denoted by $i=b$ (bubbles). V_i is the bubble or spike penetration velocity. ρ_i denotes the density. β is the model constant for the buoyancy production and C_d is the drag coefficient. Note that

$$V_i\equiv\frac{dh_i}{dt},$$

where h_i denotes the instantaneous width of the mixing region.

The choice of specific surface and volume ratios leads to the apparent variation in the form of the basic buoyancy-drag models applied by many investigators. For example, the variation in forms applied by Youngs [19], by Dimonte and Schneider [22], and by Shvarts and co-workers [7,23]. We take particular note, however, of two recent refinements. The work by Cheng, Glimm, and Sharp [23] illustrates existence of a compelling universality in the theory. Their buoyancy-drag model fits all available data, including the limit of $A=1$. This model also requires only a single numerical parameter (independent of Atwood number, for all $A<0.8$). The model also predicts, for most values of A, RMI data in terms of RTI bubble data for most values of A. Shvarts and coworkers [42,43] have shown that a buoyancy-drag model, similar to that proposed by Youngs [19], but using the coefficients from the $A=1$ Layzer model [16], can be used to study the difference in the dynamics of development for 2D and 3D instability surface evolution.

Now in the case of a single, dominant length scale, the turbulent kinetic energy equations for bubbles and spikes become

$$K_i=\frac{1}{2}V_i^2, \tag{2}$$

and the buoyancy production is

$$G_i\propto V_i g. \tag{3}$$

From the buoyancy-drag model, we have

$$V_i\frac{DV_i}{Dt}=\beta V_i Ag(t)-C_d\frac{\rho_i}{\rho_1+\rho_2}\frac{V_i^2}{h_i}|V_i|, \tag{4}$$

with the empirical introduction of coefficients βA to the buoyancy production and $C_d\rho_i/(\rho_1+\rho_2)$ to the dissipation rate term. The turbulent length scale introduced by the surface and volume ratio, L, must, from dimensional similarity, be proportional to the only outer length scale apparent in the process, h_i, the mixing zone amplitude for either bubbles for spikes.

Assuming that the effects represented by these terms can be neglected in the developing stage before mixing transition to turbulence, Eq. (4) reduces to

$$\frac{DK}{Dt}=G-D\frac{K^{3/2}}{L}. \tag{5}$$

Using the assumption (in the context of a buoyancy-drag model) that there is a single, dominant length scale, we shall show a useful parallel between the buoyancy-drag model and the one-equation transport model.

B. After mixing transition with broad band spectrum

Mode coupling (nonlinear interactions) effects broaden the spectrum of length scales. Velocity shear between the spikes and bubbles then leads to Kelvin-Helmholtz instabilities, which further broaden the spectrum of scales creating higher spatial frequencies. At large Reynolds numbers a full range of scales develops from sizes comparable to the size of the system all the way down to those of the Kolmogorov viscous dissipation scale.

One-equation turbulence models were developed to provide for the computation of the specific turbulent kinetic energy K and to account for some limited nonlocal and historic effects in the determination of the turbulent transport coefficient (eddy viscosity, ν_T). The transport equation is written [11,24,25] as

$$\frac{\partial K}{\partial t}+\overline{u}_i\frac{\partial K}{\partial x_i}=G-\tau_{ij}\frac{\partial \overline{u}_i}{\partial x_j}-\varepsilon+\frac{\partial}{\partial x_i}\left(\frac{\nu_T}{\sigma_k}\frac{\partial K}{\partial x_j}\right)+\nu\nabla^2 K. \tag{6}$$

Here $\overline{u}_i$ is the mean velocity, G is a source (other than mean shear), σ_k is a dimensionless constant, and ν is the kinematic viscosity. The production of kinetic energy resulting from the Reynolds stress $\tau_{ij}=\overline{u_i u_j}$ is the second term on the right hand side (RHS). In single point, one equation transport model closure, the Reynolds stress is related to the eddy viscosity by

$$\tau_{ij}=-\nu_T\left(\frac{\partial \overline{u}_i}{\partial x_j}+\frac{\partial \overline{u}_j}{\partial x_i}\right), \tag{7}$$

where the eddy viscosity ν_t is assumed to have the form

$$\nu_T=K^{1/2}L. \tag{8}$$

Here L is the dominant length scale. Hence, a closed system is obtained once L is specified empirically or is varied as a parameter in a systematic investigation (namely, a two-equation model [11,24,25]).

To illustrate a parallel with the buoyancy-drag model, one eliminates the following.

(1) the production from the mean shear (second term on the RHS);

(2) the turbulence transport term, which is customarily modeled based on a gradient transport hypothesis (the fourth term on the RHS);

(3) the last term on the RHS, the effect of viscous dissipation.

We also note that

(4) $D/Dt=\partial/\partial t+\overline{u}_i\partial/\partial x_i$ denotes the substantial derivative;

(5) the turbulent dissipation term, the third term on the RHS, is modeled as

$$\varepsilon=D\frac{K^{3/2}}{L}, \tag{9}$$

where D is a dimensionless constant that can be determined by experimental measurements [52] or direct numerical simulations [53,54].

The buoyancy-drag model and calculated results from its use may thereby be seen as a preliminary stage. It possesses a direct link (including definition of initial and boundary conditions) to familiar models for computation in the post-transitional turbulent mixing stages. The specific link and association is here made to the familiar hierarchy of successive levels of first order, single point closure, Reynolds-averaged turbulent transport models [11,24,25]. This correspondence with the one-equation transport model and well-established route to succeeding levels of hierarchical model refinement suggests a systematic procedure for including multiple length scale effects after mixing transition (for example, by the two-equation transport model [26]).

VI. SUMMARY AND DISCUSSION

A key finding from the present work is the suggestion that a new approach should be adopted in considering transitional flows induced by acceleration driven hydrodynamic instabilities. Of particular importance is the observation that the condition for achieving mixing transition to turbulence in the unsteady flows, including those associated with most high energy density compressible flow experiments, is quite different from the fixed Reynolds number almost universal criterion found for stationary flows. In fact this stationary flow Reynolds-number criterion is a necessary but not a sufficient mixing transition condition for unsteady flows. Essentially, we find that a sufficient condition for unsteady flow mixing transition is reached when the minimum of the laminar diffusion layer and the Liepmann-Taylor microscale dimension grows to exceed the dimension of the inner viscous microscale. In effect, this criterion for mixing transition, in general, is temporally flow dependent, since both the outer scale and the outer-scale Reynolds number are temporally flow dependent.

The temporal criterion for turbulent mixing transition from laminar (albeit unstable laminar) multifluid flow is particularly significant when one reviews the (always unsteady) flow conditions in energetic, high density experimental efforts to recreate astrophysical environments. For example, recently, it has been established that a wide range of phenomena relevant to supernova mixing may be addressed in a laser target interaction facility [29,36,37]. Despite the difficulties in experimentally attaining mixing transition to fully developed turbulence in the extremely short duration of laser driven flows, these experiments provide novel flow and state environments for astrophysical studies [55,56]. They are unique sources for ultrahigh pressure and temperature state and transport information, which together with the elevated Reynolds-number flow and almost arbitrary target material selection freedom make this class of experiments ideal for these applications. Note, however, that the experimental con-

-ditions associated with the target interaction using intensely energetic laser beams brings in several novel issues from plasma physics, which must be thoroughly understood and appreciated in interpreting the results and applying our mixing transition criterion. These issues and attendant diagnostic and interpretive considerations together with applications of our temporal transitional criterion and model procedure are discussed in a separate publication [29].

ACKNOWLEDGMENTS

This work was performed under the auspices of the U.S. Department of Energy by the University of California, Lawrence Livermore National Laboratory under Contract No. W-7405-Eng-48. We thank Dr. W. Cabot for his assistance in generating Fig. 3 based on the University of Arizona Richtmyer-Meshkov experimental data (Ref. [28]).

[1] Lord Rayleigh, Proc. R. Math. Soc. **14**, 170 (1883); Philos. Mag. **6**, 697 (1911).
[2] G. I. Taylor, Proc. R. Soc. London, Ser. A **201**, 192 (1950).
[3] R. D. Richtmyer, Commun. Pure Appl. Math. **13**, 297 (1960).
[4] E. E. Meshkov, Izv. Acad. Sci., USSR Fluid Dyn., **4**, 101 (1969).
[5] S. Chandrasekhar, *Hydrodynamic and Hydromagnetic Stability* (Dover, New York, 1961).
[6] D. H. Sharp, Physica D **12**, 3 (1984); M. Brouillette, Annu. Rev. Fluid Mech. **34**, 445 (2002).
[7] D. Shvarts, O. Sadot, D. Oran, A. Rikanati, and U. Alon, in *Handbook of Shock Waves*, (Academic Press, San Diego, 2000), Vol. 2.
[8] G. K. Batchelor, *The Theory of Homogeneous Turbulence* (Cambridge University Press, New York, 1953).
[9] A. S. Monin and A. M. Yaglom, *Statistical Fluid Mechanics* (MIT Press, Cambridge, MA, 1975), Vol. 2.
[10] H. Tennekes and J. L. Lumley, *First Course in Turbulence* (MIT Press, Cambridge, MA, 1972).
[11] S. B. Pope, *Turbulent Flows* (Cambridge University Press, New York, 2000).
[12] D. Chapman, AIAA J. **17**, 1293 (1979).
[13] S. G. Saddoughi and S. V. Veeravalli, J. Fluid Mech. **268**, 333 (1994).
[14] A. W. Cook and Y. Zhou, Phys. Rev. E **66**, 026312 (2002); Y. Zhou, Phys. Fluids A **5**, 1092 (1993); Y. Zhou, *ibid.* **5**, 2511 (1993); D. O. Martinez, S. Chen, G. D. Doolen, L. P. Wang, and Y. Zhou, J. Plasma Phys. **57**, 195 (1997); Y. Zhou and C. G. Speziale, Appl. Mech. Rev. **51**, 267 (1998); Y. Zhou, P. K. Yeung, and J. G. Brasseur, Phys. Rev. E **53**, 1261 (1996).
[15] P. E. Dimotakis, J. Fluid Mech. **409**, 69 (2000).
[16] D. Layzer, Astrophys. J. **122**, 1 (1955).
[17] M. J. Lighthill, *An Informal Introduction to Theoretical Fluid Mechanics* (Oxford University Press, Oxford, UK, 1986).
[18] R. Clift, J. R. Grace, and M. E. Weber, *Bubbles, Drops and Particles* (Academic, New York, 1978).
[19] J. C. Hanson, P. A. Rosen, T. J. Goldsack, K. Oades, P. Fieldhouse, N. Cowperthwaite, D. L. Youngs, N. Mawhinney, and A. J. Baxter, Laser Part. Beams **8**, 51 (1990).
[20] J. Werne, Phys. Rev. E **49**, 4072 (1994).
[21] D. Shvarts, U. Alon, D. Oran, R. L. McCrory, and C. P. Verdon, Phys. Plasmas **2**, 2465 (1995).
[22] G. Dimonte and M. Schneider, Phys. Rev. E **54**, 3740 (1996); G. Dimonte, Phys. Plamas **7**, 2255 (2000).
[23] B. Cheng, J. Glimm, and D. H. Sharp, Phys. Lett. A **268**, 366 (2000).
[24] C. G. Speziale, Annu. Rev. Fluid Mech. **23**, 107 (1991).
[25] D. C. Wilcox, *Turbulence Modeling for CFD* (DCW Industries, La Canada, California, 1993).
[26] Y. Zhou, G. B. Zimmerman, and E. W. Burke, Phys. Rev. E **65**, 056303 (2002); Y. Zhou, R. Rubinstein, D. Eliason, and W. Cabot, Astron. Astrophys. (to be published).
[27] S. B. Dalziel, P. F. Linden, and D. L. Youngs, J. Fluid Mech. **399**, 1 (1999).
[28] M. A. Jones and J. W. Jacobs, Phys. Fluids **9**, 3078 (1997); B. D. Collins and J. W. Jacobs, J. Fluid Mech. **464**, 113 (2002); J. W. Jacobs and V. V. Krivets, in *Proceedings of the 23rd International Symposium on Shock Waves*, edited by F. Lu (University of Texas at Arlington Press, 2001).
[29] H. F. Robey, Y. Zhou, A. C. Buckingham, P. Keifer, B. A. Remington, and R. P. Drake, Phys. Plasmas **10**, 614 (2003).
[30] Y. Zhou *et al.*, Phys. Plasmas **10**, 1883 (2003).
[31] G. G. Stokes, Mathematics & Physics Papers, 3 (Cambridge University Press, London, 1901), pp. 1–141.
[32] H. Lamb, *Hydrodynamics* (Dover, New York, 1911), pp. 619–620.
[33] H. Schlichting, *Boundary-Layer Theory* (McGraw-Hill, New York, 1951).
[34] J. G. Clerouin, M. H. Cherfi, and G. Zerah, Europhys. Lett. **42**, 37 (1998).
[35] C. Paquette, C. Pelletier, C. Fontaine, and G. Michaud, Astrophys. J., Suppl. Ser. **61**, 177 (1986).
[36] B. A. Remington, R. P. Drake, H. Takabe, and D. Arnett, Phys. Plasmas **7**, 1641 (2000).
[37] H. F. Robey, J. O. Kane, B. A. Remington, R. P. Drake, O. A. Hurricane, H. Louis, R. J. Wallace, J. Knauer, P. Keiter, D. Arnett, and D. D. Ryutov, Phys. Plasmas **8**, 2446 (2001).
[38] A. W. Cook and P. Dimotakis, J. Fluid Mech. **443**, 69 (2001).
[39] V. A. Andronov, S. M. Bakahrakh, E. E. Meshkov, V. N. Mokhov, V. V. Nikiforoc, A. V. Pevnitskii, and A. I. Tolshmyakov, Sov. Phys. JETP **44**, 424 (1976); D. L. Youngs, Physica D **12**, 32 (1984); D. L. Youngs, *ibid.* **37**, 270 (1989); K. I. Reed, *ibid.* **12**, 45 (1984).
[40] Y. Zhou, Phys. Fluids **13**, 538 (2001).
[41] U. Alon, J. Hecht, D. Ofer, and D. Shvart, Phys. Rev. Lett. **72**, 534 (1995).
[42] D. Shvarts, D. Oron, D. Kartoon, A. Rikanati, O. Sadot, Y. Srebro, Y. Yedvab, D. Ofer, A. Levin, E. Sarid, G. Ben-Dor, L. Erez, G. Erez, A. Yosef-Hai, U. Alon, and L. Arazi, in *Inertial Fusion Sciences and Applications*, edited by C. Labaune, W. J. Hogan, and K. A. Tanaka (Elsevier, Paris, 1999).
[43] D. Oron, L. Arazi, D. Kartoon, A. Rikanati, U. Alon, and D. Shvarts, Phys. Plasmas **8**, 2883 (2001).
[44] G. I. Barenblatt, in *Nonlinear Dynamics and Turbulence*, ed-

ited by G. I. Barenblatt, G. Loos, and D. D. Joseph (Pitman, Boston, 1983).
[45] D. L. Youngs, Laser Part. Beams **12**, 725 (1994).
[46] J. D. Ramshaw, Phys. Rev. E **58**, 5834 (1998).
[47] T. Clark and Y. Zhou (private communication).
[48] O. Sadot, L. Erez, U. Alon, D. Oron, L. A. Levin, G. Erez, G. Ben-Dor, and D. Shvarts, Phys. Rev. Lett. **80**, 1654 (1998).
[49] Q. Zhang and S. I. Sohn, Phys. Fluids **9**, 1109 (1997).
[50] G. L. Brown and A. Roshko, J. Fluid Mech. **64**, 775 (1974).
[51] D. Papamoschou and A. Roshko, J. Fluid Mech. **197**, 453 (1988).
[52] K. R. Sreenivasan, Phys. Fluids **27**, 867 (1984).
[53] P. K. Yeung and Y. Zhou, Phys. Rev. E **56**, 1746 (1997).
[54] K. R. Sreenivasan, Phys. Fluids **10**, 528 (1998).
[55] L. Smarr, J. R. Wilson, R. P. Barton, and R. L. Bowers, Astrophys. J. **246**, 511 (1981).
[56] W. D. Arnett, J. N. Bahcall, R. T. Kirshner, and S. E. Woosley, Annu. Rev. Astron. Astrophys. **27**, 629 (1989).